

Integrated Ferroelectrics

An International Journal

ISSN: 1058-4587 (Print) 1607-8489 (Online) Journal homepage: <https://www.tandfonline.com/loi/ginf20>

Evaluation of Structural Properties of Calcium Hexaferrites on the Basis of Synthesis Method

Ch. Mamatha

To cite this article: Ch. Mamatha (2020) Evaluation of Structural Properties of Calcium Hexaferrites on the Basis of Synthesis Method, Integrated Ferroelectrics, 204:1, 23-32, DOI: [10.1080/10584587.2019.1674982](https://doi.org/10.1080/10584587.2019.1674982)

To link to this article: <https://doi.org/10.1080/10584587.2019.1674982>



Published online: 24 Jan 2020.



Submit your article to this journal [↗](#)



View related articles [↗](#)



View Crossmark data [↗](#)



Evaluation of Structural Properties of Calcium Hexaferrites on the Basis of Synthesis Method

Ch. Mamatha

Department of Physics, Sri Venkateshwara College of Engineering, Bangalore, India

ABSTRACT

In the new age of technologies, the necessity of new magnetic materials inspired researchers to carry the study on hexagonal ferrites largely due to their extensive applications as magnetic materials. Ferrites have become vital for both commercial and technological usages. Their applications are based on very basic properties viz., saturation magnetization, high electrical resistivity, low electrical losses and chemical stability. Diminution to nanosize, unique and technologically thought-provoking properties have been obtained. On the other hand, nanoparticles could be modified with various structures by different synthesis methods and substitutions to enhance their properties. Most common applications are magnetic recording, data storage materials, ferrofluids and drug delivery. In the present work, aluminum substituted calcium hexaferrite nanoparticles were successfully synthesized in two different methods visualized as solution combustion and hydrothermal synthesis to attain elite results. Structural properties are characterized by XRD, SEM and TEM. XRD data of all the samples have confirmed the formation of single-phase M-type hexagonal ferrites with the space group of $P6_3/mmc$. Grain size, lattice parameters and volume of the samples are calculated. SEM analysis revealed that the particles are of uniform grain morphology and nano in size. Although the compound is same, based on the synthesis method structural properties are found to be different. Particle size and shape are different in two methods.

ARTICLE HISTORY

Received 1 October 2018
Accepted 12 August 2019

KEYWORDS

Hexaferrite; combustion;
hydrothermal

1. Introduction

Ferrites are large class of oxides with excellent magnetic properties, which have been investigated and applied for the past few decades. The formation of the hexagonal ferrites is an extremely complex process. Methodologies to formulate hexagonal ferrites are pretty complex in nature. Despite several investigations by many researchers over the years, the right and simplified methods have not been derived [1–4]. Currently, to prepare hexagonal ferrite nanoparticles, various synthesis methods such as chemical coprecipitation [5], hydrothermal [6], sol–gel [5–7], solution combustion synthesis [8], etc. have been developed. In the present work, calcium hexaferrites substituted with trivalent Al ions are synthesized in two different methods such as hydrothermal and solution combustion. Their structural properties are studied and reported.

CONTACT Ch. Mamatha  mamathasree@yahoo.co.in

Color versions of one or more of the figures in the article can be found online at www.tandfonline.com/ginf.

© 2019 Taylor & Francis Group, LLC

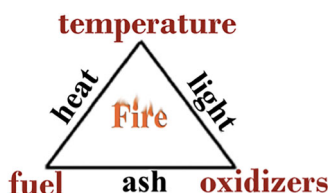


Figure 1. Combustion process.

Ferrimagnetic oxides or ferrites are ceramic ferrimagnetic materials which are dark brown or gray in appearance and very hard and brittle in character. They are prepared by heat-treating the various transition metal oxides or alkaline earth oxides with the ferric oxides. The magnetic behavior exhibited by the ferrites is called ferrimagnetism, which is quite different from ferromagnetism that is exhibited by metallic substances. Substituted hexaferrites belonging to the family of magnetoplumbite with general formula $M(Fe_{12}O_{19})$ where M is usually barium, strontium, calcium or lead, are fascinating due to their specific magnetic behavior. The basic structure consists of 38 oxygen ions occupying the interstitial sites forming a close packed hexagonal structure. Twenty-four ferric ions occupy five different locations in the unit cell in which $2a$, $4f_2$ and $12k$ are octahedral, $4f_1$ is tetrahedral and $2b$ is bi-pyramidal [9,10].

In the current scenario, hydrothermal synthesis is gaining significance as a relatively convenient way of making hexaferrite nanoparticles. In hydrothermal synthesis a solution of metal salts and a base are autoclaved under pressure to give the final product. The product is often a mixed phase containing unreacted precursors, and sometimes Fe_2O_3 , which are removed by washing with dilute HCl [11].

Combustion synthesis is also known as self-propagating high temperature synthesis (SHS). To ignite the process, an oxidizer, a fuel, and the right temperature are needed. All these three essentials make up a fire triangle as shown in Figure 1. Fire can be described as an abandoned combustion, which produces heat, light, and ash [1]. The process makes use of highly exothermic redox chemical reactions between an oxidizer and a fuel [11].

2. Experimental

A series of M-type aluminum substituted calcium hexaferrites with general formula $CaAl_xFe_{12-x}O_{19}$ ($x = 0, 1, 2, 3, 4$) are prepared successfully in two different methods, hydrothermal and combustion, to study structural properties.

2.1. Hydrothermal Synthesis

To prepare samples in hydrothermal method, stoichiometric quantities of the AR grade $Ca(NO_3)_2 \cdot 4H_2O$, $Fe(NO_3)_3 \cdot 9H_2O$, $Al(NO_3)_3 \cdot 9H_2O$ and NaOH were used as reactants. Reactants were dissolved in deionized water under vigorous stirring. The solution was poured into Teflon liner held in a stainless steel autoclave, sealed and kept in the oven at $160^\circ C$. Same temperature was maintained for 18 h. After cooling the autoclave to room temperature in natural process, the precipitate obtained was separated by centrifugation gives the calcium ferrite, ionic state of sodium nitrate and water. By repeatedly

washing with ethanol and deionized water in sequence removes the sodium and nitrate ions. The solution was then dried in hot air oven at 80 °C for 3 h. [Figure 2](#) shows the flow of hydrothermal synthesis.

2.2. Solution Combustion Synthesis

The flow of the combustion synthesis is shown in [Figure 3](#). Samples are prepared with AR grade calcium nitrate $\text{Ca}(\text{NO}_3)_2 \cdot 4\text{H}_2\text{O}$, iron nitrate $\text{Fe}(\text{NO}_3)_3 \cdot 9\text{H}_2\text{O}$, aluminum nitrate $\text{Al}(\text{NO}_3)_3 \cdot 9\text{H}_2\text{O}$ and freshly prepared oxalyl dihydrazide ODH ($\text{C}_2\text{H}_6\text{N}_4\text{O}_2$)

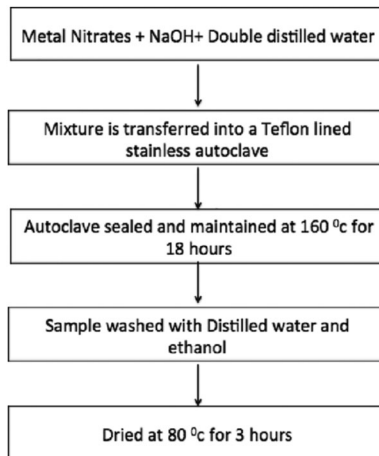


Figure 2. Flow of hydrothermal synthesis.

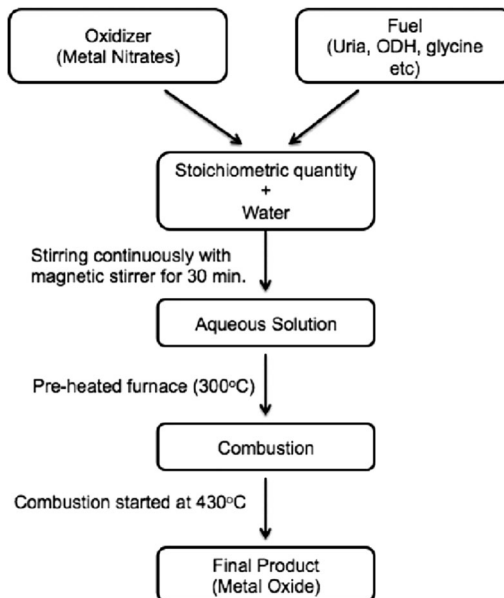


Figure 3. Flow of combustion synthesis.

[12,13]. In solution combustion method, stoichiometric amounts of metal nitrates act as an oxidizing agent and fuel (oxalyl dihydrazide (ODH) $[C_2H_6N_4O_2]$) acts as reducing agent with exothermic reaction. Metal nitrates along with ODH dissolved completely in double distilled water to form an aqueous solution. Combustion process is performed in a muffle furnace and samples are calcined at $900^\circ C$ [14].

3. Structural Studies

Structural studies are carried out on powder X-ray diffractometer with step size of 0.2° in 2° range of 20° – 80° at RT. The PXRD pattern of Calcium hexaferrites substituted with aluminum is shown in Figures 4 and 5. X-ray diffraction studies confirm the formation of hexaferrites with the space group $P6_3/mmc$.

The average particle size, D , was determined from line broadening of (107) reflection using Scherrer [3] formula given by

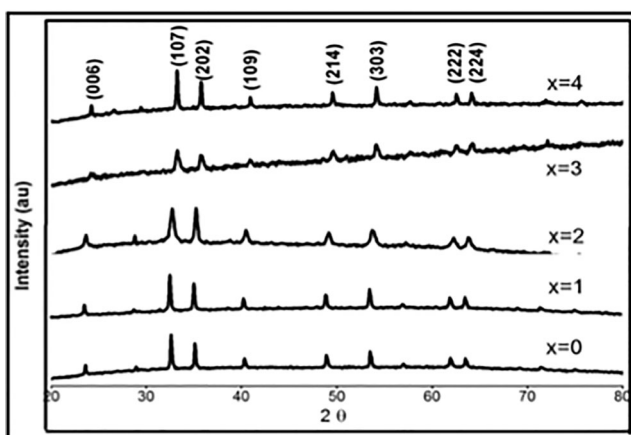


Figure 4. XRD spectrum of samples prepared in hydrothermal synthesis.

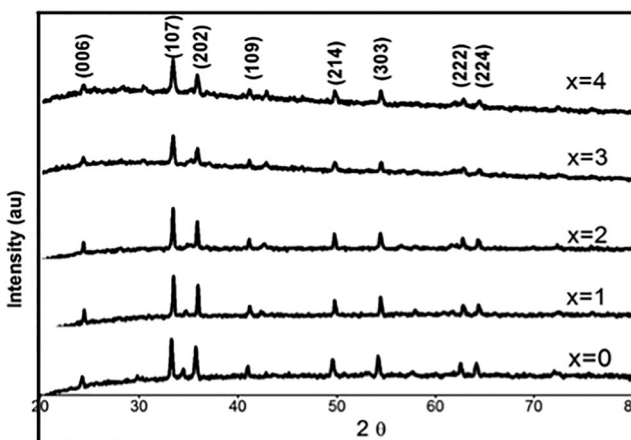


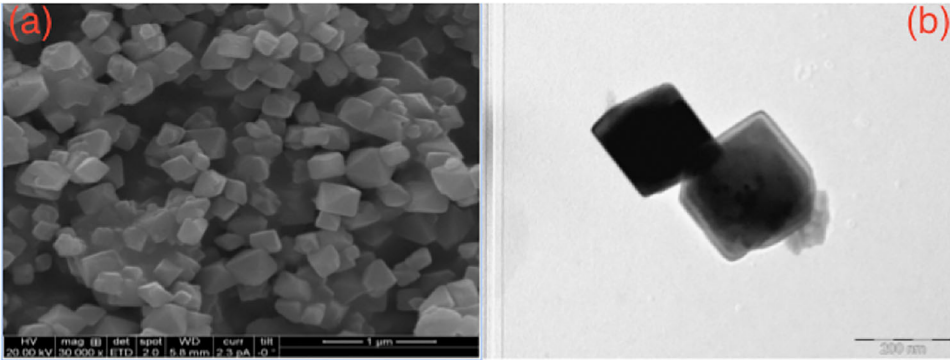
Figure 5. XRD spectrum of samples prepared in combustion synthesis.

Table 1. Structural parameters the samples prepared in combustion synthesis.

Sample	Grain size, D (nm)	Lattice parameters		Volume of the cell, V (\AA^3)	c/a
		a (\AA)	c (\AA)		
CaFe ₁₂ O ₁₉	33.43	5.809	22.342	652.89	3.85
CaFe ₁₁ AlO ₁₉	30.47	5.803	22.287	649.94	3.84
CaFe ₁₀ Al ₂ O ₁₉	32.59	5.805	22.253	649.39	3.83
CaFe ₉ Al ₃ O ₁₉	30.8	5.986	21.823	677.18	3.64
CaFe ₈ Al ₄ O ₁₉	23.4	5.979	21.949	679.50	3.67

Table 2. Structural parameters the samples prepared in hydrothermal synthesis.

Sample	Grain size, D (nm)	Lattice parameters		Volume of the cell, V (\AA^3)	c/a
		a (\AA)	c (\AA)		
CaFe ₁₂ O ₁₉	41.38	5.998	22.856	712.08	3.81
CaFe ₁₁ AlO ₁₉	37.61	5.995	22.851	711.22	3.81
CaFe ₁₀ Al ₂ O ₁₉	19.53	5.993	22.844	710.52	3.81
CaFe ₉ Al ₃ O ₁₉	13.36	5.806	22.394	653.74	3.86
CaFe ₈ Al ₄ O ₁₉	38.2	5.816	22.368	655.23	3.85


Figure 6. (a) SEM and (b) TEM images of CaFe₁₂O₁₉ prepared in hydrothermal synthesis.

$$D = \frac{K \lambda}{\beta \cos \theta} \quad (1)$$

where β is the angular line width at half maximum intensity and θ the Bragg angle of the height peak. Structural properties, such as lattice parameters (a , c), particle size (D), volume (V) and c/a ratios are calculated by using following equations [15].

$$\frac{1}{d^2} = \frac{4(h^2 + hk + k^2)}{3a^2} + \frac{l^2}{c^2} \quad (2)$$

$$V_{\text{cell}} = 0.866a^2c \quad (3)$$

4. Results and Discussions

X-ray diffraction spectrum for all the samples prepared in both hydrothermal synthesis and combustion synthesis are shown in [Figures 4](#) and [5](#). X-ray diffraction studies

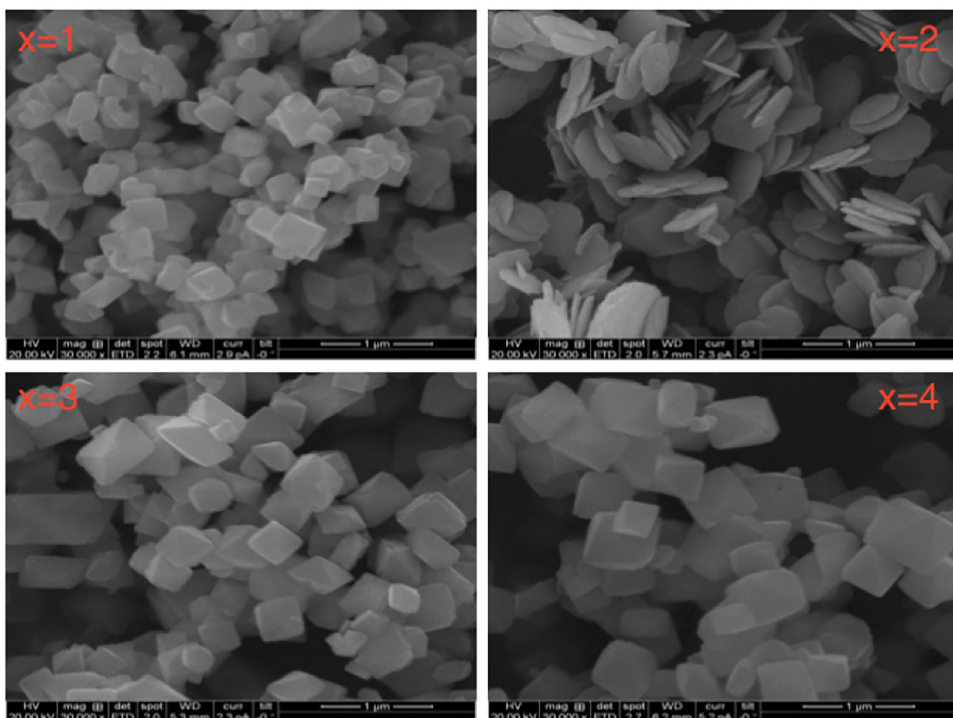


Figure 7. SEM images of $\text{CaAl}_x\text{Fe}_{12-x}\text{O}_{19}$.

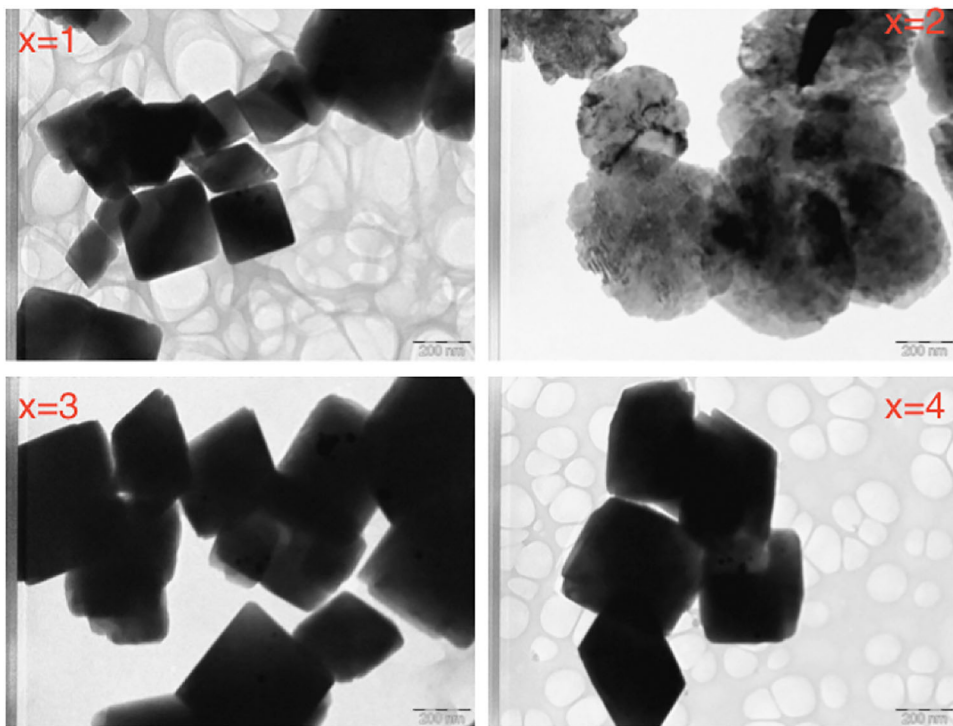


Figure 8. TEM images of $\text{CaAl}_x\text{Fe}_{12-x}\text{O}_{19}$.

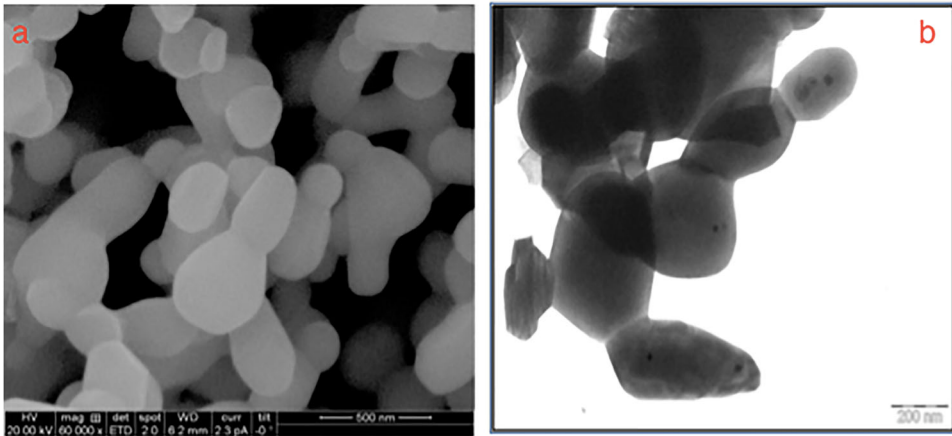


Figure 9. (a) SEM and (b) TEM images of $\text{CaFe}_{12}\text{O}_{19}$ prepared in combustion synthesis.

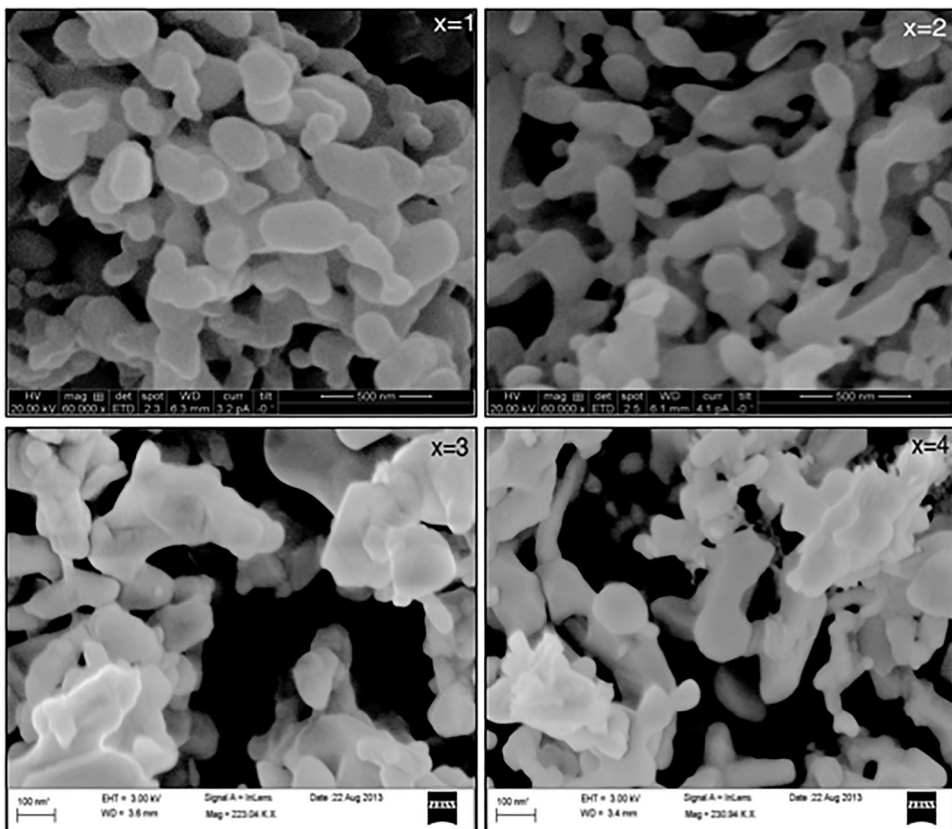


Figure 10. SEM images of $\text{CaAl}_x\text{Fe}_{12-x}\text{O}_{19}$ prepared in combustion.

confirm the formation of hexaferrites with the space group $\text{P6}_3/\text{mmc}$. The major intensity diffraction peaks of samples have been found at (006), (107), (202), (109), (214), (303), (222) and (224) orientations as mentioned in Figures 4 and 5. All peaks

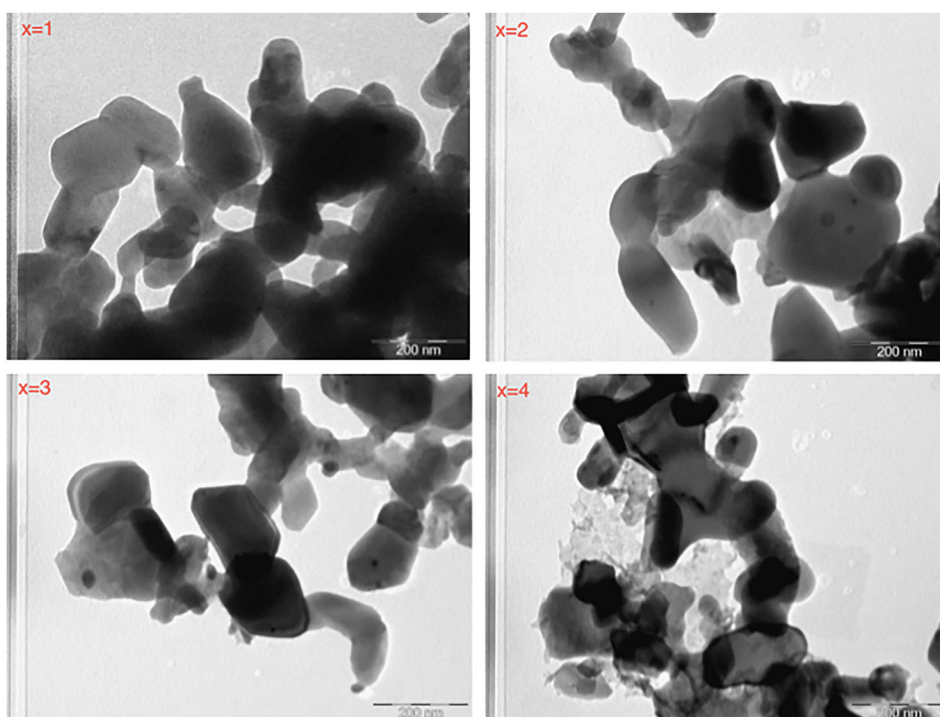


Figure 11. TEM images of $\text{CaAl}_x\text{Fe}_{12-x}\text{O}_{19}$ in combustion.

match perfectly with Bragg reflections of the hexagonal structure with space group $P6_3/mmc$ and matching with the PCPDF no. 49-1586. A close examination of the PXRD pattern indicates slight variation in the parameters such as peak intensities, peak positions and peak width, with the increase in the aluminum content due to the small ionic radius of Al^{3+} ion (0.54 \AA) than Fe^{3+} (0.65 \AA). Al^{3+} Substitution for Fe^{3+} causes the shrinkage of crystal lattice [9,16–18]. Structural properties, such as lattice parameters (a , c), particle size (D), volume (V) and c/a ratios are given in Tables 1 and 2. There is a variation in the particle size with different substitution. The lattice parameters ratio c/a lies in the range from 3.67 to 3.85 for the samples prepared in combustion synthesis and 3.81 to 3.85 for samples prepared in hydrothermal synthesis, exhibited the formation of M-type hexagonal structure [9,16]. Consequently, the aberrance of the crystal lattice leads to the changes in the crystal lattice parameters a , c and variation in the radius of the crystal grains. M-type hexaferrite structure is assumed if the lattice parameters ratio is observed to be lower than 3.98 [17–19].

Figures 6–8 show SEM and TEM images of the samples prepared in hydrothermal synthesis. Figures 9–11 show SEM and TEM images of the samples prepared in combustion synthesis. From figures it is evident that particles are in nanosize. Agglomeration increases with the increase of substitution. It clearly shows that particle size and shape are entirely different for the same compound in two different methods.

5. Conclusions

Series of Al substituted calcium hexaferrites with general formula $\text{CaAl}_x\text{Fe}_{12-x}\text{O}_{19}$ ($x = 0, 1, 2, 3, 4$) have been prepared by two different synthesis methods, hydrothermal synthesis and combustion synthesis. The role of synthesis method in structural properties and substitution of Al^{+3} in place of Fe^{+3} are studied and summarized.

Powders are characterized by XRD, SEM and TEM. X-ray diffraction patterns reveal the formation of M-type hexagonal structure with space group $\text{P6}_3/\text{mmc}$. Though the compound $\text{CaAl}_x\text{Fe}_{12-x}\text{O}_{19}$ is same, structural properties are varied widely as the methodologies are different. The average particle size is found to be in the nano range in both methods. Size and shape of the particles are more effective in hydrothermal synthesis as compared to combustion synthesis.

References

1. D. Lisjak and M. Drogenik, Synthesis and characterisation of A-Sn-substituted ($A = \text{Zn}, \text{Ni}, \text{Co}$) BaM-hexaferrite powders and ceramics, *J. Eur. Ceram. Soc.* **24** (6), 1841 (2004). DOI: [10.1016/S0955-2219\(03\)00445-X](https://doi.org/10.1016/S0955-2219(03)00445-X).
2. S. Singhal, A. N. Garg, and K. Chandra, Evolution of the magnetic properties during the thermal treatment of nanosize $\text{BaMFe}_{11}\text{O}_{19}$ ($M = \text{Fe}, \text{Co}, \text{Ni}$ and Al) obtained through aerosol route, *J. Magn. Magn. Mater.* **285** (1–2), 193 (2005). DOI: [10.1016/j.jmmm.2004.07.039](https://doi.org/10.1016/j.jmmm.2004.07.039).
3. R. C. Pullar, Hexagonal ferrites: A review of the synthesis, properties and applications of hexaferrite ceramics, *Prog. Mater. Sci.* **57** (7), 1191 (2012). DOI: [10.1016/j.pmatsci.2012.04.001](https://doi.org/10.1016/j.pmatsci.2012.04.001).
4. J. L. Snoek, *New Developments in Ferromagnetic Materials* (Elsevier Publishing Co., Inc., New York, Amsterdam, 1947).
5. V. Adelskold, Arkiv Kemi Min. Geol X-ray studies on magneto-plumbite, $\text{Pb}_{0.6}\text{Fe}_{12}\text{O}_{13}$, and other substances resembling “beta-alumina”, *12/A/29*, 1938.
6. J. F. Wang *et al.*, A study of Pr-substituted strontium hexaferrite by hydrothermal synthesis, *J. Alloys. Compd.* **403** (1–2), 104 (2005). DOI: [10.1016/j.jallcom.2005.05.025](https://doi.org/10.1016/j.jallcom.2005.05.025).
7. L. Junliang *et al.*, One-step synthesis of barium hexaferrite nano-powders via microwave-assisted sol-gel auto-combustion, *J. Eur. Ceram. Soc.* **30** (4), 993 (2010). DOI: [10.1016/j.jeurceramsoc.2009.10.019](https://doi.org/10.1016/j.jeurceramsoc.2009.10.019).
8. J. Huang, H. Zhuang, and W. Li, Optimization of the microstructure of low-temperature combustion-synthesized barium ferrite powder, *J. Magn. Magn. Mater.* **256** (1–3), 390 (2003). DOI: [10.1016/S0304-8853\(02\)00973-3](https://doi.org/10.1016/S0304-8853(02)00973-3).
9. D. K. Kulkarni and C. S. Prakash, Structural and magnetic properties of $\text{CaAl}_4\text{Fe}_8\text{O}_{19}$, *Bull. Mater. Sci.* **17** (1), 35 (1994). DOI: [10.1007/BF02747632](https://doi.org/10.1007/BF02747632).
10. H. Kojima and K. Goto, Proceeding of Inter Conference on Ferrites, Center for Academic publication, Japan, 198, p. 335.
11. K. C. Patil *et al.*, *Chemistry of Nano Crystalline Oxides: Combustion Synthesis, Properties and Applications* (World Scientific Publishing Co, Singapore, 2008).
12. Ch. Mamatha *et al.*, Structural, electrical and magnetic properties of aluminum substituted nanocalcium hexaferrites, *Int. J. ChemTech Res.* **6** (3), 2165 (2014).
13. Ch. Mamatha, P. Subhashini, and M. Krishnaiah, Effect of cobalt substitution on electrical properties of calcium hexaferrite nano particles, *Arch. Appl. Sci. Res.* **7** (6), 7 (2015).
14. Ch. Mamatha *et al.*, Structural and electrical properties of aluminium substituted nano calcium ferrites, *Procedia Mater. Sci.* **5**, 780 (2014). DOI: [10.1016/j.mspro.2014.07.328](https://doi.org/10.1016/j.mspro.2014.07.328).
15. Ch. Mamatha, M. Krishnaiah, and C. S. Prakash, Comparative study of $\text{CaAl}_3\text{Fe}_9\text{O}_{19}$ and $\text{CaAl}_4\text{Fe}_8\text{O}_{19}$ nanoparticles synthesized by solution combustion method, in *Proceedings of the Second National Seminar on New Materials Research and Nanotechnology*, Ooty (2013), pp. 135–138.

16. C. S. Prakash *et al.*, Substitutional effect of magnetic behaviour in calcium hexaferrite, *J. Magn. Magn. Mater.* **140–144**, 2089 (1995). DOI: [10.1016/0304-8853\(94\)01409-4](https://doi.org/10.1016/0304-8853(94)01409-4).
17. M. F. Din *et al.*, Influence of Cd substitution on structural, electrical and magnetic properties of M-type barium hexaferrites co-precipitated nanomaterials, *J. Alloys Compd.* **584**, 646 (2014). DOI: [10.1016/j.jallcom.2013.09.043](https://doi.org/10.1016/j.jallcom.2013.09.043).
18. V. Blanco-Gutierrez *et al.*, Neutron diffraction study and superparamagnetic behavior of ZnFe₂O₄ nanoparticles obtained with different conditions, *J. Solid State Chem.* **184** (7), 1608 (2011). DOI: [10.1016/j.jssc.2011.04.034](https://doi.org/10.1016/j.jssc.2011.04.034).
19. Ch. Mamatha, M. Krishnaiah, and B. Sreedhar, Enhancement of magnetic properties of calcium hexaferrites with aluminium substitution, *Procedia Eng.* **215**, 130 (2017). DOI: [10.1016/j.proeng.2017.11.001](https://doi.org/10.1016/j.proeng.2017.11.001).